



Towards Improving the “Detection” Power of Brain Imaging Experiments Using fNIRS*

Li Zhu, Maria Peifer, and Laleh Najafizadeh

Department of Electrical and Computer Engineering, Rutgers University



Introduction

• Functional Near-infrared spectroscopy (fNIRS) is a non-invasive functional brain imaging technique which uses light in the range of 690 to 1000 nm to measure the local changes in the cerebral concentrations of oxygenated hemoglobin and deoxygenated hemoglobin associated with brain activity [1].

• Studies which target localizing the brain regions related to a specific activity (i.e. “detection” studies), generally involve block-design experiments. The recorded signals across blocks under the same condition are then averaged, using the conventional arithmetic averaging technique, and the related activated areas are then identified. As there might be occasions during the experiment, in which the onset of hemodynamic responses are not time-locked across multiple blocks of the same type, (due to subject distraction for example), use of conventional arithmetic technique may result in not correctly identifying the activation regions (e.g. the averaged amplitude is decreased). The inaccuracy of arithmetical averaging is an essential problem and of great concern because it might lead to misunderstanding of the brain functionality.

• In this study, we introduce an averaging method based on dynamical time warping (DTW) algorithm [2] which helps to improve the accuracy of the averaged signal across multiple blocks, and hence, increases the detection power. The technique is applied to real experimental fNIRS data and results are compared with the conventional averaging technique.

fNIRS Technique

In a typical functional brain imaging experiment using NIRS technique, an array of detectors and low power NIR light sources are placed on the head. The light entering at a source position and exiting the head at a detector position samples a diffuse volume along this path. Due to the low optical absorption of biological tissue at NIR wavelengths, NIR light can penetrate deep enough to sample the outer 1.5–2 cm of the head through skin and skull and reach the outer approximately 5–10 mm of the brain tissue.

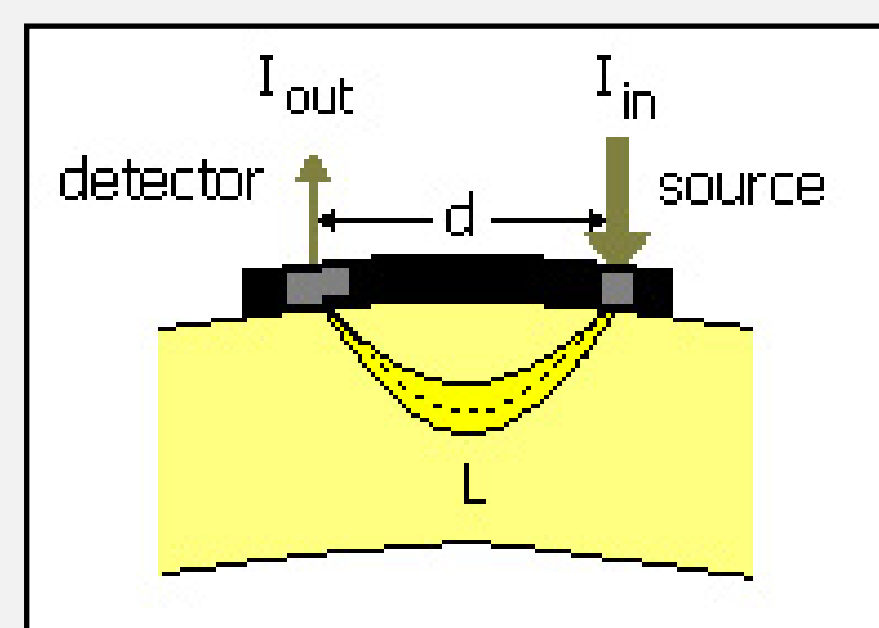


Fig. 1: Propagation path of the NIRS light.

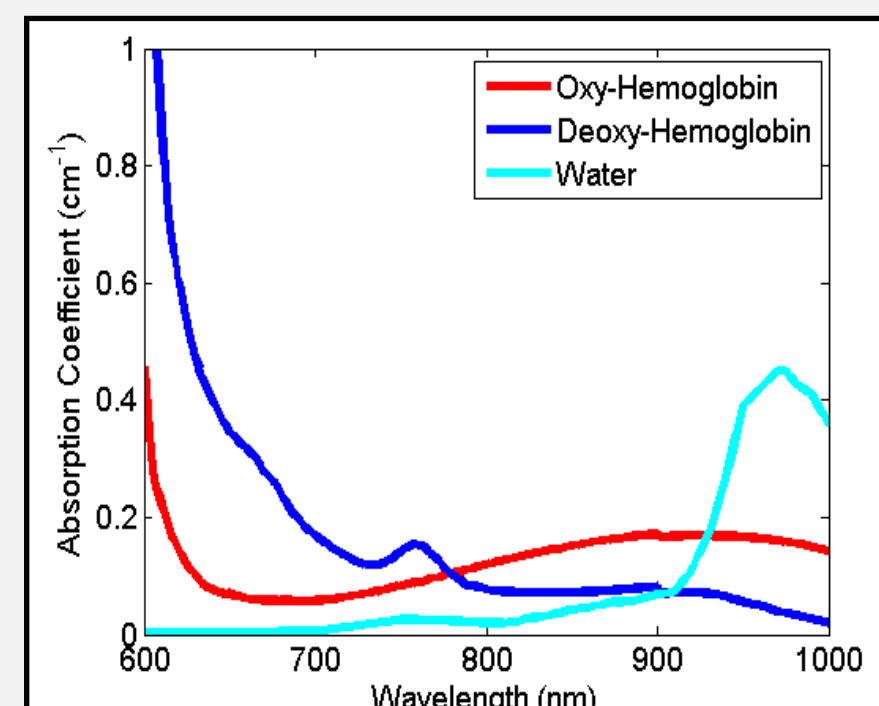


Fig. 2: Absorption spectra for Oxy and Deoxy Hemoglobin in the Near-Infrared range [3].

Changes in the concentrations of oxygenated and deoxygenated hemoglobin can be extracted using Modified Beer Lambert law:

$$\ln \left(\frac{I_{2,\lambda_1}}{I_{1,\lambda_1}} \right) = -\Delta\mu_{a,\lambda_1} DPF \cdot x = -(\epsilon_{HbO_2,\lambda_1} \Delta C_{HbO_2} + \epsilon_{HbR,\lambda_1} \Delta C_{HbR}) DPF_{\lambda_1} \cdot x$$

$$\ln \left(\frac{I_{2,\lambda_2}}{I_{1,\lambda_2}} \right) = -\Delta\mu_{a,\lambda_2} DPF \cdot x = -(\epsilon_{HbO_2,\lambda_2} \Delta C_{HbO_2} + \epsilon_{HbR,\lambda_2} \Delta C_{HbR}) DPF_{\lambda_2} \cdot x$$

Experimental Setup

- 5 healthy volunteers
- 17 sources, 16 detectors
- 52 channels
- 695 nm and 830 nm
- Sampling rate: 10 Hz
- Spatial Resolution: 3 cm
- Stimuli sent by E-prime

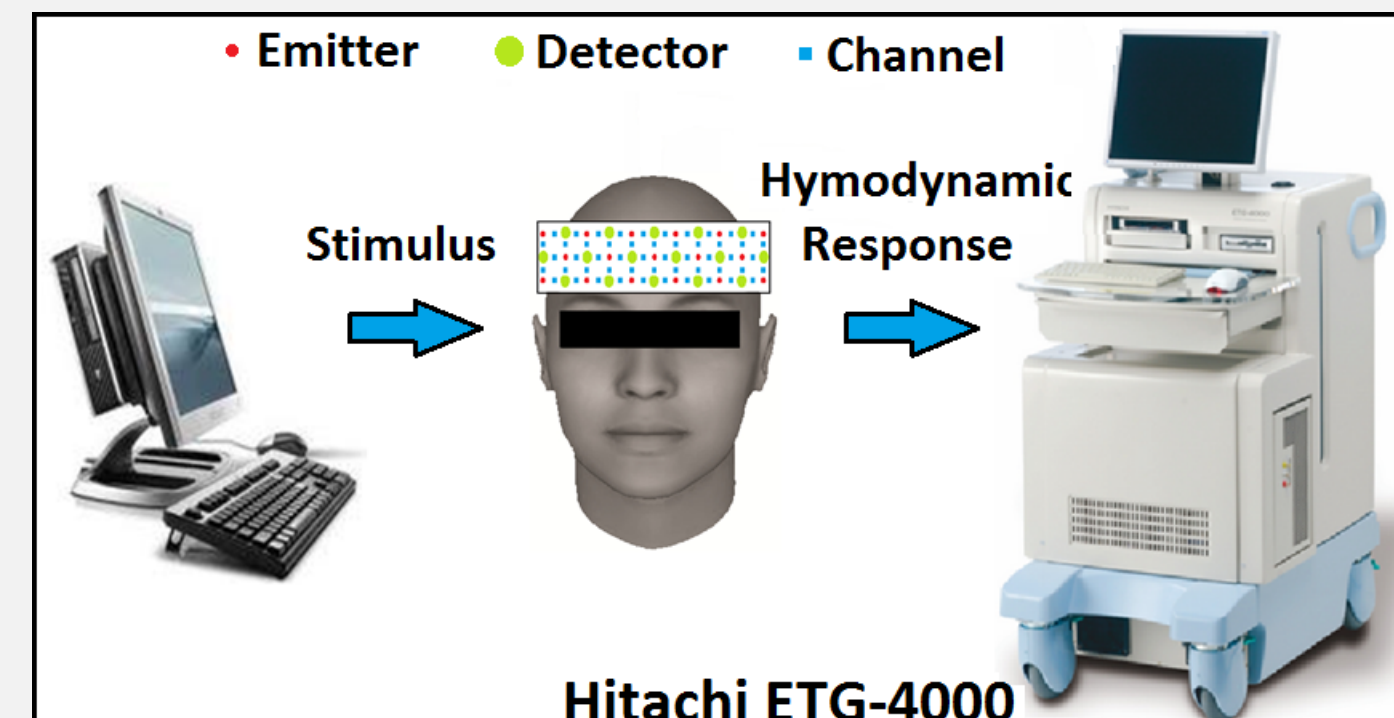


Fig. 3: Experimental setup.

Paradigm

N-Back (N=0, 1, 2, 3)

- 3 blocks for each N-Back
- 16-stimuli in each block
- Presentation time=1.8 s
- ITI=0.2 s
- Left click if see target

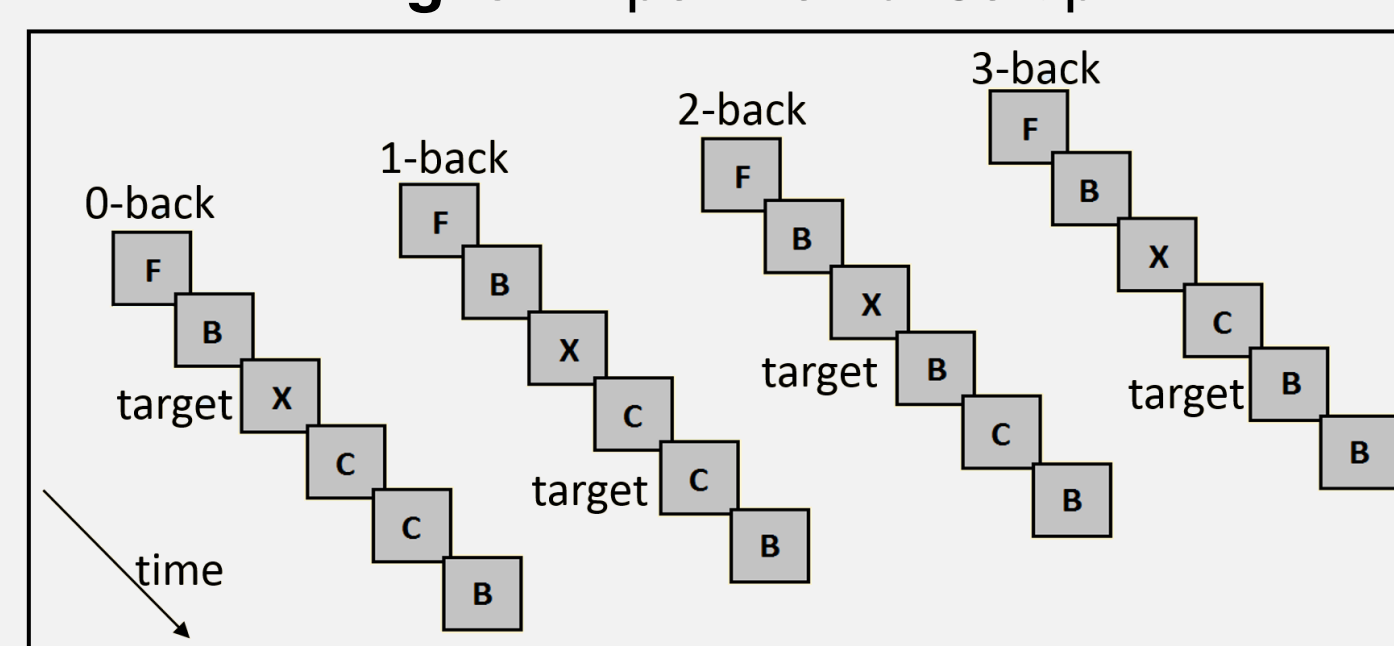


Fig. 4: Experimental paradigm.

Pre-processing

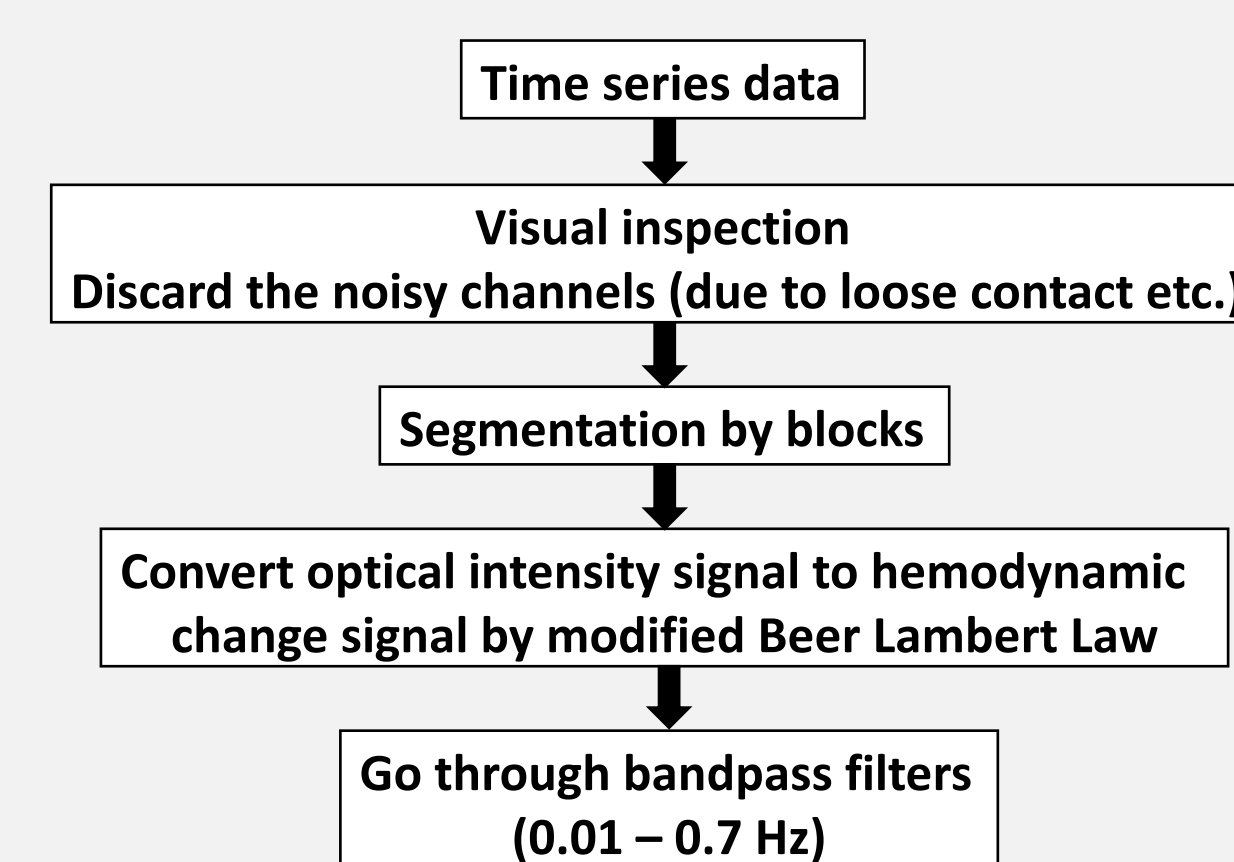


Fig. 5: Flowchart for pre-processing.

DTW Base

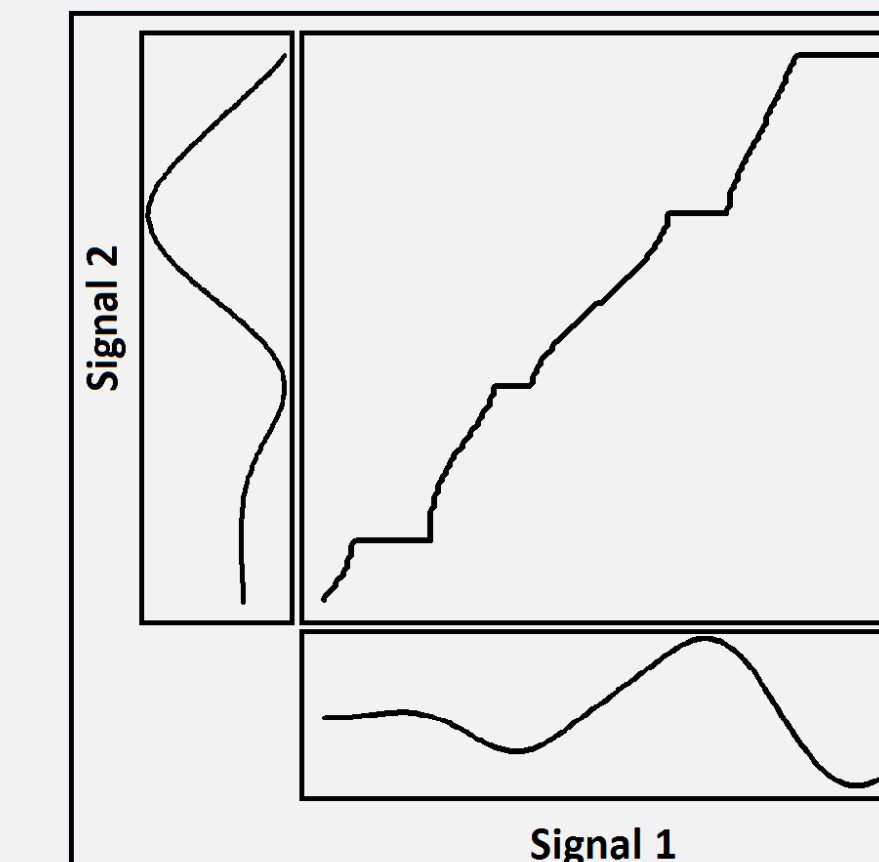


Fig. 6: Alignment between two signals [4].

Method

To illustrating the method, we demonstrate the way to average over three signals from one channel. We denote signal from block 1 as b_1 , block 2 as b_2 and block 3 as b_3 , arithmetic averaged signal of b_1 , b_2 and b_3 as c ,

- **Step 1:** find arithmetic average c for b_i ($i=1,2,3$).
- **Step 2:** form distance matrices for the pair of c and b_i ($i=1,2,3$), respectively.
- **Step 3:** find the optimal warping path w_i ($i=1,2,3$).
- **Step 4:** align c , b_i from w_i ($i=1,2,3$), re-assign the value of each point in c as the arithmetic average of its associated points in b_i ($i=1,2,3$).

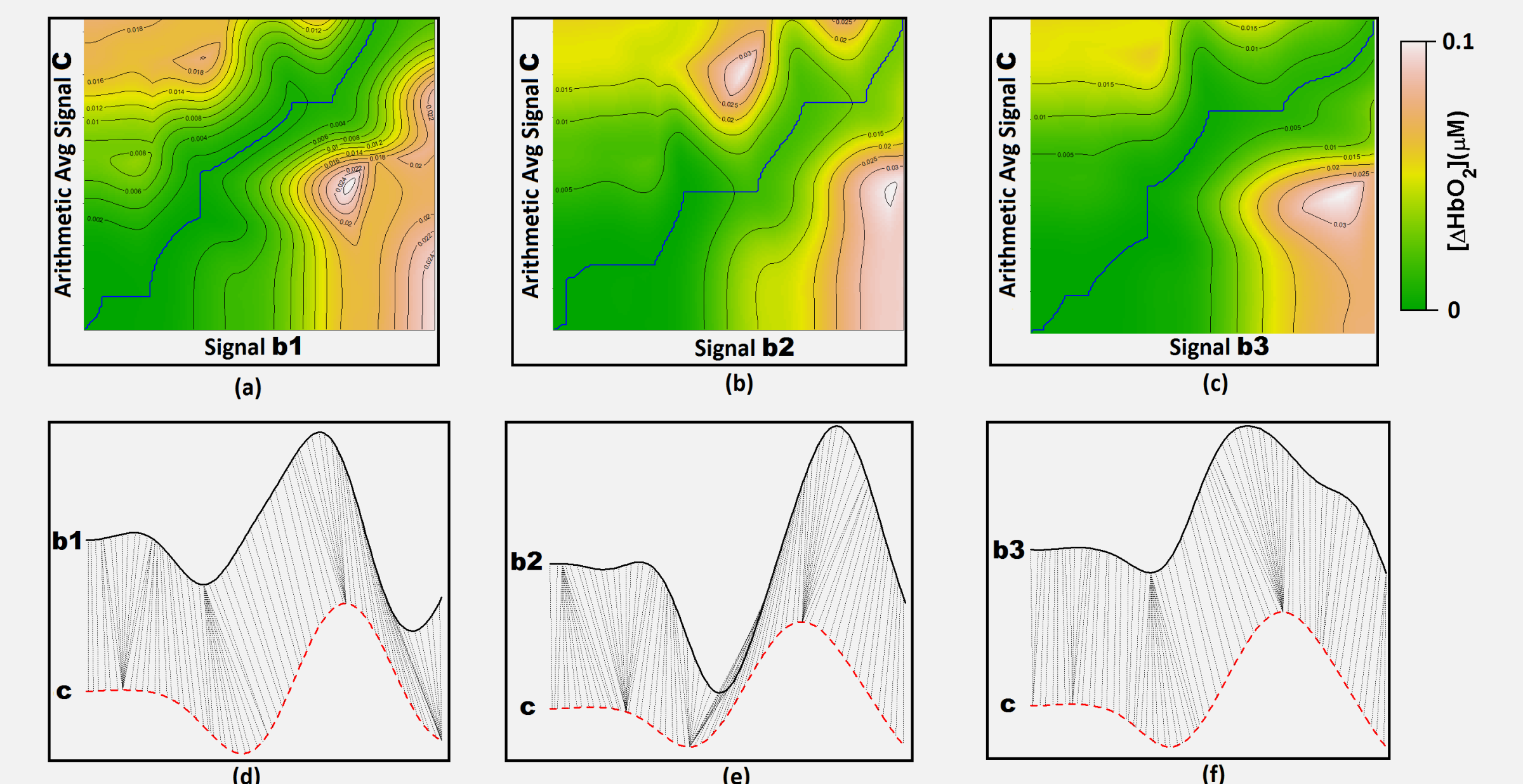


Fig. 7: The illustration of the distance matrices and signal alignment. (a) – (c) demonstrate the optimal warping path between c and b_i ($i=1,2,3$). The contour maps represent the distance landscape, brown color represents large distance and green color represents low distance. The blue lines represent the warping path. Alignment visualization for c and b_i are plotted in (d) – (f) respectively. The associated point-pairs are connected with segments.

Results and Discussions

The performance comparison of conventional and DTW averaging is evaluated according to within group sum of squares (WGSS) [2]. The percentage improvement in WGSS is calculated from:

$$\% \text{Improvement in WGSS} = \frac{WGSS_{\text{arithmetic avg}} - WGSS_{\text{DTW avg}}}{WGSS_{\text{arithmetic avg}}} \times 100.$$

Dataset	Mean of WGSS Improvement (%)	Variance of WGSS Improvement
ΔHbO_2 0-back	9.37	0.0026
ΔHbO_2 1-back	0.64	3.5480×10^{-9}
ΔHbO_2 2-back	14.99	0.0041
ΔHbO_2 3-back	16.72	0.0055
ΔHbR 0-back	0.46	1.5590×10^{-9}
ΔHbR 1-back	7.33	7.4626×10^{-4}
ΔHbR 2-back	4.99	2.2267×10^{-4}
ΔHbR 3-back	5.12	4.7479×10^{-4}

Table 1: % WGSS improvement for 8 datasets from one subject.

Discussions: Block averaging of hemodynamic responses is an important step in activity detection studies. Conventional averaging techniques may fail to accurately identify the activation regions due to possible existing misalignment in the recorded hemodynamic response from each block. In this paper, we addressed this problem for fNIRS signals by using DTW averaging technique. The comparison was made for all four experimental conditions and for both ΔHbO_2 and ΔHbR signals. An improvement of up to 16% in accuracy was obtained using the DTW method.

References

[1] Amyot, F. et al., "Normative database of judgment of complexity task with functional near infrared spectroscopy—Application for TBI." Neuroimage, 60, pp. 879-883, 2012.
 [2] F. Petitjean, et. al., "A global averaging method for dynamic time warping, with applications to clustering," Pattern Recognition, Vol. 44.3, pp. 678-693, 2011.

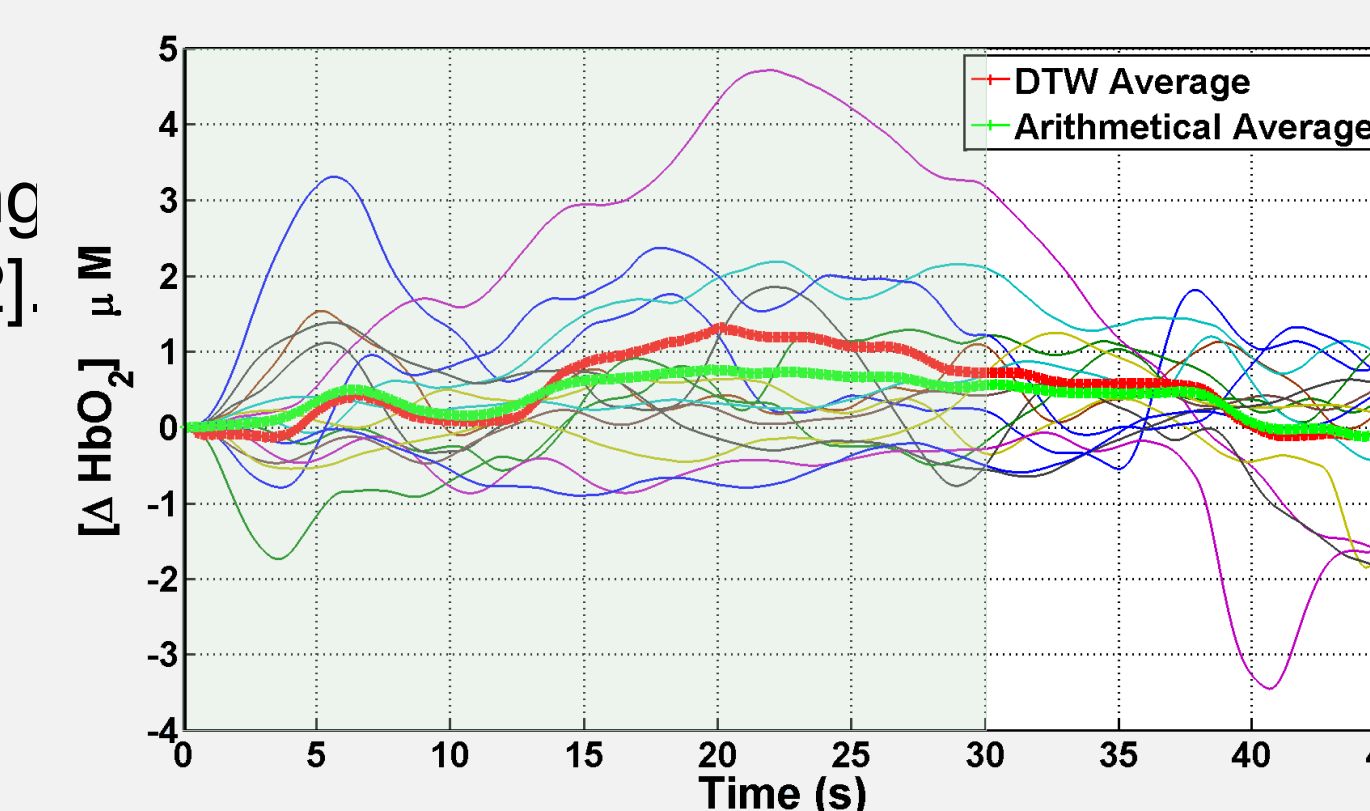


Fig. 8: Performance comparison between DTW and arithmetic averaging over all subjects for ΔHbO_2 from Channel 8 and 3-back tasks. The shaded area represents the experimental block duration.

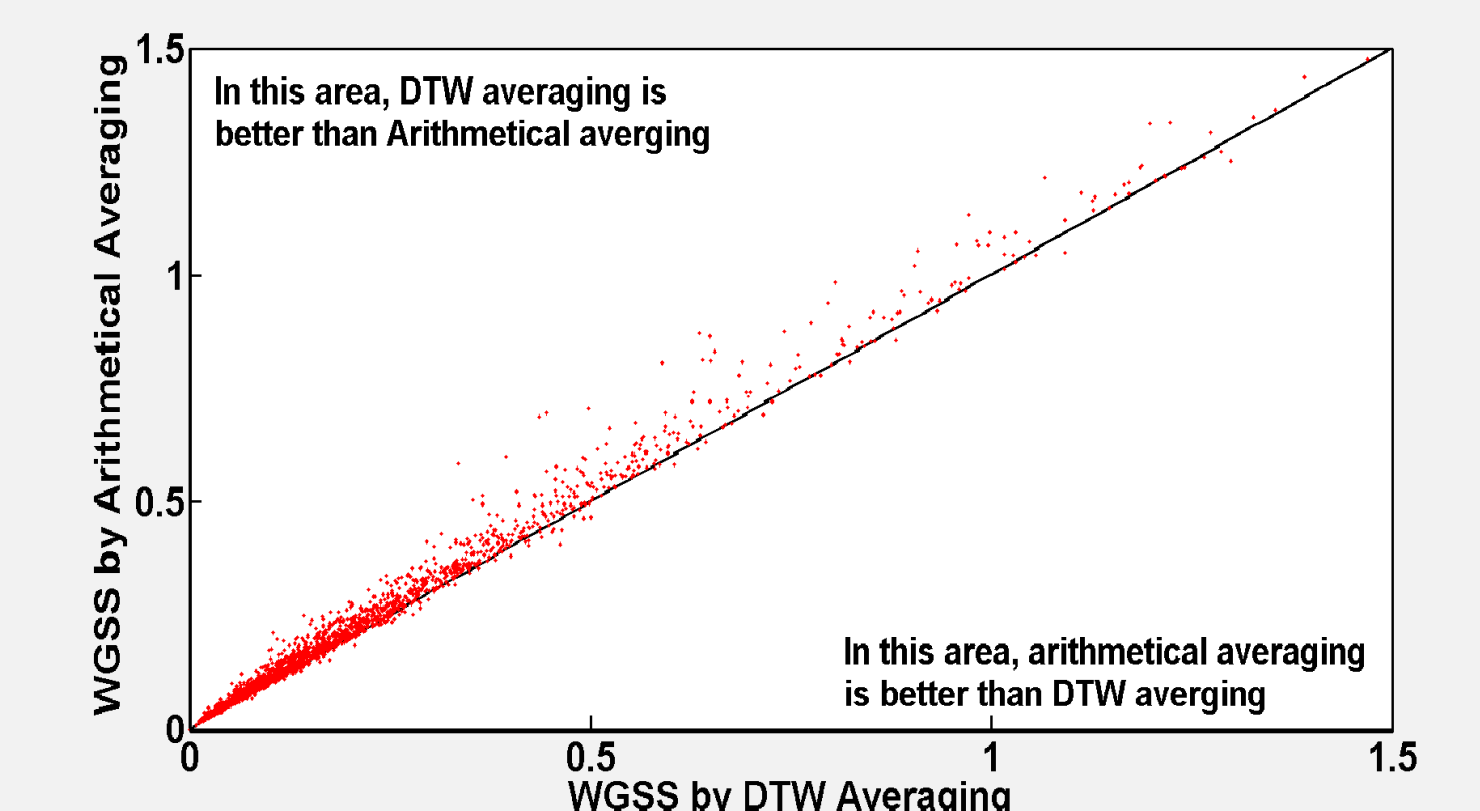


Fig. 9: WGSS by DTW averaging vs. arithmetical averaging, across all 5 subjects, 52 channels, and 4 experimental conditions.